MoroccanJournal of Chemistry
ISSN: 2351-812X
http://revues.imist.ma/?journal=morjchem&page=login
Elmiz & al./ Mor. J. Chem. 7 N°2 (2019) 242-253

Synthesis and Characterization of CPC Organo-modified and Al_{13} Pillared Modified Bentonite.

Elmiz Mohamed[1], ESSIFI Kamal[1], SALHI Samira[1], BERGAYA Faiza[2] and TAHANI Abdesselam[1]

[1] *LACPRENE; Université Mohamed 1er; Route de Sidi Maâfa; BP 524-Oujda- Morocco.*
[2] *ICMN (UMR 7374 CNRS), Université d'Orleans, 1B, Rue de la Ferollerie, 45071 Orleans, France*

*** Corresponding author:**
elmiz.mohamed@gmail.com
Received 15 Nov 2018,
Revised 12 March ,
Accepted 15 May 2019.

Abstract

In this study, a Moroccan bentonite was used to prepare three modified clays: a sodic clay (B-Na) prepared from raw clay by sodium exchange process. The homo-ionic sodium clay was then used to prepare an organoclay (B-CPC) by intercalation of cetyl-pyridinium chloride (CPC) and an aluminum-pillared clay (Al-PILC) by intercalation of hydroxyl-aluminum cations. The FT-IR analysis showed that the pillaring with Al13 and intercalation with CPC did not destroy the initial structure of the sodium bentonite, and some characteristic bands of the intercalating agents appears. Detailed characterization with azote gas adsorption confirmed that the specific surface area of the natural bentonite was 70 m2/g,and 107 m2/g for the B-Na when impurities are eliminated and exchanged with sodium cations. The total surface area for the Al-PILC pillared bentonite was significantly higher than that of unpillared samples and reached the value of 270 m2/g resulting in the increase of the adsorption sites for the N2 gas. A considerable decrease to 7 m2/g of the total surface area for the B-CPC organophilic bentonite was observed. The B-CPC was the clay that showed the highest (XRD) value of interlayer distance (21.7 Å) corresponding to the bilayer intercalated between the clay mineral layers, and Al-PILC have a XRD peak at 19.4 Å which corresponds to the Al13 intercalating pillars.

Keywords: Bentonite; Montmorillonite; Organoclay; Pillared clay; Cationic surfactant; Hydroxyl aluminum.

1. Introduction

In recent years, material sciences have involved studies related to the production of materials having a controlled pore structure in order to improve porous materials found in nature.Several porous materials have been used as adsorbents, such as activated carbon, zeolite, fly ash, clay minerals, bio-sorbents, and certain metal oxides based composites[1].

Due to its high cation exchange capacity, swelling properties and large sheets, montmorillonite clay has an important place in the production of porous materials especially by modification. This modification processis based on a mechanism of cationic exchange in which robust inorganic or organic cations are introduced in the interlinear space of the clay. This process, besides making possible the insertion of active phases, confers greater thermal and mechanical stability to the material, greater exhibition of the active sites and an increment in the superficial area [2].The agent introduced and the preparation conditions have important effects on the quality of modified clay [3-7]. The modification of clays with aluminum (Pillaring clay) is considered to be an ion exchange process of the main pillaring agent $[Al_{13}O_4\ (OH)_{24}\ (H_2O)_{12}]^{7+}$, called the Keggin or Al_{13} ions [8, 9]. It was confirmed through the X-Ray Diffraction Analysis, that the intercalation of aluminum polycations Al_{13} with a basal spacing (interlayer spacing) of about 18 Å at room temperature resulted in transforming them into Al_2O_3 oxide after calcination at 500 °C. The intercalated species act as props (pillars) that keep the clay layers apart and prevent them from collapsing under vacuum, at higher temperatures, or under specific conditions [10]. Thus, the bridging process generates micro and meso-porosity in the inter-lamellar spaces of clays, which are also called nanomaterials. Pillared clays have remarkable adsorption properties that are related both to geometric characteristics of the porous spaces, and to specific interactions of the pillars and the clay layers [10]. Adsorption and pH-dependent ion exchange capacities of PILCs have been extensively studied [11-18]. These modified clay minerals (PILCs) were used in attempt to improve Controlled Release Formulations of Pesticides [19]. Furthermore, the adsorption properties of PILCs on active molecules such as Thymol have been recently studied for its application to reversible encapsulation [20].Therefore, these pillared clays are not effective adsorbents to remove hydrophobic organic compounds in an aqueous system. When the organic cations are used for intercalation into clays, the resulting materials are denoted as organoclays [21]. Organoclays can be prepared by exchanging the inorganic cations of the clay surface by organic cations containing long hydrocarbon chains such as hexa-decyl-tri-methyl ammonium chloride (HDTMA) cation, [22] cetyl-pyridinium chloride [23], and the like.

Different surfactants were used to prepare organic clays. These include single and double cationic surfactants [24-27], active anionic cationic surfactants [28] and nonionic surfactants [29]. Organic clays formed, however, are structurally different even when the same surfactant was used under similar experimental conditions [30, 31]. These results suggest that both the surfactant and the clay affect the structure and properties of the resultant organoclays. These intercalated organic cations may extend the inter-laminar layer of the clay and form a pseudo-organic phase, which increases the sorption capacity of hydrophobic organic compounds in water.These hydrophobic clays have attracted much interest because they have found wide applications as adsorbents of organic pollutants [32-35]. As components in the synthesis of Nano-composite clay-based polymers [36], and as precursors in the preparation of meso-porous materials[13]. The pillared clays or organoclays are achieved using smectite clays like montmorillonite or bentonite.

The studied Bentonite clay was taken from the deposits of Azzouzete in the district of Nador (Morocco) at 20 Km south of Nador city (35’01’ 56,49° N and 2’52’ 11,37°O with 106 m of Altitude). The aim of this study is to contribute to the possibilities of valorization process of these bentonites [37]. The objective of this investigation is to prepare and characterize three modified clays of Nador bentonite by different intercalating agents; a sodic clay (B-Na) prepared from raw clay by sodium exchange process. The organoclay (B-CPC) is prepared by intercalation of cetyl-pyridinium chloride (CPC). This homo-ionic sodium clay (B-Na) is then used to prepare an aluminum-pillared clay (Al-PILC) by intercalation of hydroxyl-aluminum cations and an organoclay (B-CPC) by intercalation of cetyl-

pyridinium chloride (CPC). The characterization is performed by means of X-Ray diffraction, Infrared spectroscopy, thermal analyses, surface area and pore structure determinations. These properties are directly related to the effectiveness of these materials for specific industrial use.

2. Methodology.

2-1.Purification and Preparation of Sodium Bentonite.

In this method, a mass of 1 Kg of raw clay is dispersed in 5 liters of distilled water with a solid/liquid ratio: 1/5. The mixture was stirred for an hour, until the homogenization full suspension, followed by treatment by HCl (0.5 M) to remove carbonate. The resulting mixture was washed by H_2O_2 (10%) in order to oxidize organic matter. The resulting product was then extensively washed (6 times) with NaCl 1M and centrifuged to give saturated clays. The dark grey residue in the centrifuge tube was eliminated because it contained enriched fraction in impurity (quartz, cristobalite, feldspar …) The samples were then washed and dialyzed against distilled water, until the conductivity in the dialysis bath was less than 2µS/cm. The granular fraction size ≤ 2 µm were then obtained by accurate sedimentation. The air-dried clays were gently ground to give a powder of Na-B.

2-2.Synthesis of Organo-clay (B-CPC) by Intercalation.

A suitable amount of cationic surfactant (cetyl-pyridinium chloride HIMEDA 99%) was dissolved in distilled water at a concentration of 1% of weight (10g surfactant in 1L of distilled water) that was homogenized each time before use.
The modified organoclay was prepared as described by Srinivasan and Fogler (1990) [31]. Traditional organoclay was prepared by cation exchange. Na-montmorillonite was treated with cetyl-pyridinium chloride (CPC) for an amount equivalent to more than 100% of the CEC. In order to prepare this support (CPC-montmorillonite) and homogenize it through mechanical stirring, 10g of purified sodium clay with the solution of the surfactant was stirred for about 12 hours at room temperature. Montmorillonite resulting from cetyl-pyridinium chloride (CPC-montmorillonite) was washed several times with distilled water until the excess of surfactant, which appears in the form of foam, disappears, and then it was dried at 60°C and ground into a powder before use.

2-3.Synthesis of Pillared Clay (B-Al-PILC) by Al_{13}.

The pillaring solution containing $[Al_{13}O_4\ (OH)_{24}\ (H_2O)_{12}]^{7+}$ cations was obtained by adding 250 ml of Al_{l3} (0.4 M) to 550 ml of NaOH (0.4 M) (drop by drop flow). The final neutralization ratio which is defined as $[OH]_{Tot}/[Al\ (III)]_{Tot}$ was 2.4, and the solution was stirred for 12 hours at room temperature. The resultant solution of pH = 4.5, was added to the clay suspension 2% (1 g clay/100 ml H_2O) and stirred for 6 hours at room temperature. The pillared clay form was then centrifuged, filtered and dried at 60 °C in air. Calcination was performed at 350 °C for 6 hours. The degree of intercalation of the pillaring cations was determined by X-Ray Diffraction, by analysing the variations of d (001) in oriented clay-aggregate [38].

2-4.Characterization Methods.

The natural samples purified and modified clay are subjected to analysis and identification by X-ray diffraction (XRD), infrared spectroscopy (IR) and Thermal, textural and physicochemical analysis. X-ray diffractogramswere recorded in a Shimadzu XRD diffractometer D6000 stations working on the monochromatic copper Kα1 radiation (1.54 Å). Concerning the characterization by XRD, two methods were used: non-oriented preparation and preparation of oriented plates. Infra Red (I.R) spectra were acquired using a Shimadzu Fourier Transform spectrometer over a range varying from 400 to 4000 cm^{-1} with a resolution of 2 cm^{-1}, and the samples were prepared in the form of a

dispersion in a vial KBr (1/200 by weight). Thermal analysis was carried out in a SHIMATZU D6000 coupled to a DC ampler and temperature controller. Data from DTA-TG were obtained in all cases at a heating rate of 5˚C/min between 30˚C and 1000˚C and under N_2 atmosphere. The textural characteristics of clays before and after modification were determined by two methods: First, from N_2 adsorption/desorption isotherms at 77˚K using micrometrics AS AP 2000 volumetric adsorption-desorption apparatus and surface Area and Pore size Analyzer. The BET surface areas were calculated using the multi-point method for the use of relative pressure (P/P_0) between 0.00095 and 0.9917. Second, the total surface and external and internal surface areas were determined from adsorption of ethylene glycol.

3. Results and discussion

3-1.X-ray Diffraction.

The X-Ray powders diffractograms of raw bentonite clay and exchanged bentonite clay are shown in Figure 1.

The X-ray diffraction (XRD) of the raw bentonite powder shows that the bentonite belongs to the smectites family with the reflection (001) located at 14 Å. This shows that natural bentonite is a calcium form. The presence of the peak (6.33) at d = 1.49 Å confirm the predominance of montmorillonite fraction in the clay [39]. It was also noted that there is a presence of crystalline phases in the form of impurities in Quartz (Q) d = 3.34 Å. The review of the spectrum of the exchanged purified sodium bentonite confirms a good purifying bentonite raw compared to the peak (001). The changes observed were: First, a displacement in the position of the peak (001) of 14 to 12.76 Å which indicates that the exchange process between sodium and calcium was carried out. Second, a disappearance of certain characteristic peaks of the crystalline phases in the form of impurities, especially that of quartz located at d = 3.34 Å. Third, an intensification of certain peaks corresponding to those of the montmorillonite d = 12.76 Å and d = 3.07 Å. The XRD analyses show for B-Al_{13}, a clear shift of the signal at 12.76 Å (corresponding to smectite signal for sodic bentonite), to a value close to 19.44 Å, which represents an increase in basal space of the starting B-Na clay. This indicates that the chemical modification of the clays led to a successful pillaring process. The basal spacing that expands to about 19.44 Å is equal to the thickness of one clay layer (9.4 Å) plus the height of one Al_{13} cation (9.7 Å)[40].

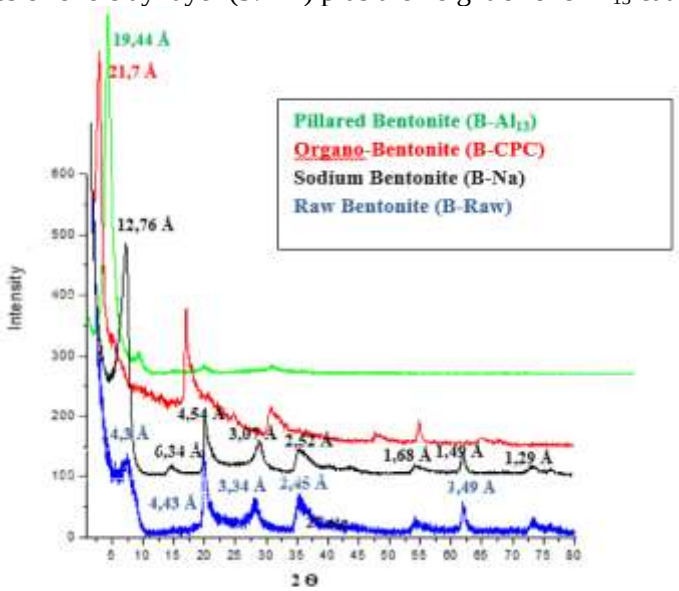

Figure 1. X-Ray powdersdiffractograms of raw Bentonite clay and exchanged Bentonite clay

The B-Na has basal spacing of 1.27 nm (2Θ = 6.94°). Compared to B-Na, the reflection of the basal B-CPC was moved downward at an angle (2Θ = 4.18°) and the corresponding basal spacing B-CPC was expanded to 2.15 nm, indicating that the CPC was successfully inserted into the B-Na. (Figure 1). The displacementof the mainreflection

from14,33Åto10 Å. The decreaseof the equidistanceis due tothe loss of theinter-foliar water. Based onthe orientation of theorganic aminein the modifiedbentonite [41, 42] , one can deduce that the CPC alkyl chains are forming a bilayer lamellar structure and relatively a small number ofCPCmolecules are intercalatedinto thebentonite interlayerspace.

3-2.Thermal Analysis (DTA & GTA).

The TGA and DTA curves for raw bentonite, exchanged sodium bentonite, pillared bentonite and organoclay bentonite are shown respectively in:Figure 2, Figure 3Figure 4 Examination of the DTA analysis curve (Figure 3) of the sodium bentonite shows, in the field of low temperatures, the existence of 104 °C intense endothermic peak. This phenomenon is linked to the starting zeolite and the hygroscopic water of bentonite. Mass loss that accompanied these thermal accidents is very important and about14.66% of the initial mass (Figure 2).

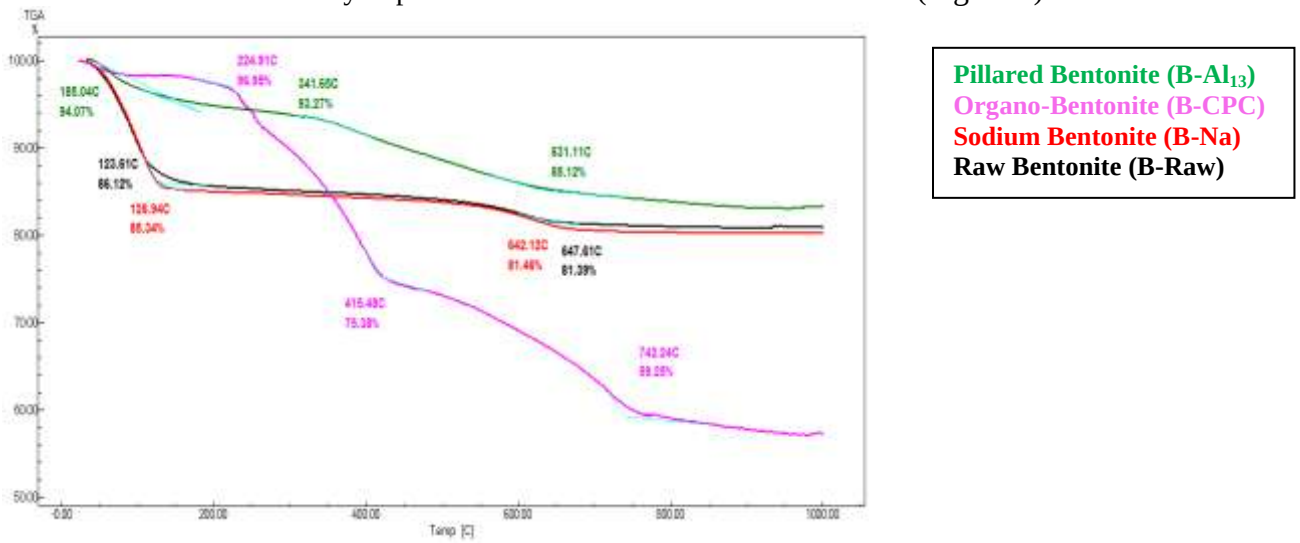

Figure 2. Gravimetric thermal analysis Results of the studied clays

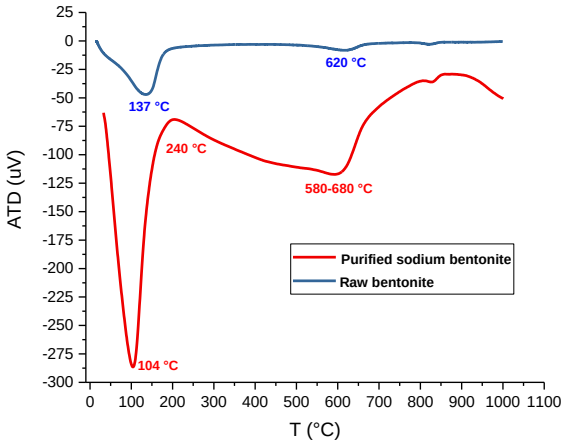

Figure 3. Differential thermal analysis (DTA) curves for Raw and sodium bentonite

Anotherendothermicpeak of low intensity occursat the temperature of618°C.This corresponds to thestartof the structuralwater removal of OHgroups bonded to theedges of theclaysheets. The total mass loss associated withthis peakis about of3.88% of weight. The DTAcurvealsoexhibits an exothermicaccidentat894.25°Cdue torecrystallizationofthebentonite. The DTA curve relating to the raw bentonite (Figure 3) presents endothermic phenomena ranges from 50°Cto240 °C. These temperature ranges correspond to the elimination of solvating water from the interlayer space of the clay and the surface of the mineral crystals of the impurities. In the second stage, the

raw bentonite exhibits a multi-step dehydroxylation between 450 and 700◦C associated to a total mass loss of about 13.88% and 4.73% of the initial mass theycorrespond respectively to thestronglyretainedwater and the structural water of bentonite and mineral crystals of the impurities. Above 800◦C, no further apparent mass loss is noted and a typical peak appears at about 858°C, mainly due to decomposition/recrystallization reactions of both bentonite and the crystal mineral impurities. Concerning the Al pillaredmaterials (PILCs (B-Al-PIL)),the netisomorphic substitutioninthe clay withdifferent bondingstrengths betweenthetracecationandthe surroundingoxygenions (or hydroxyl) can be observed.

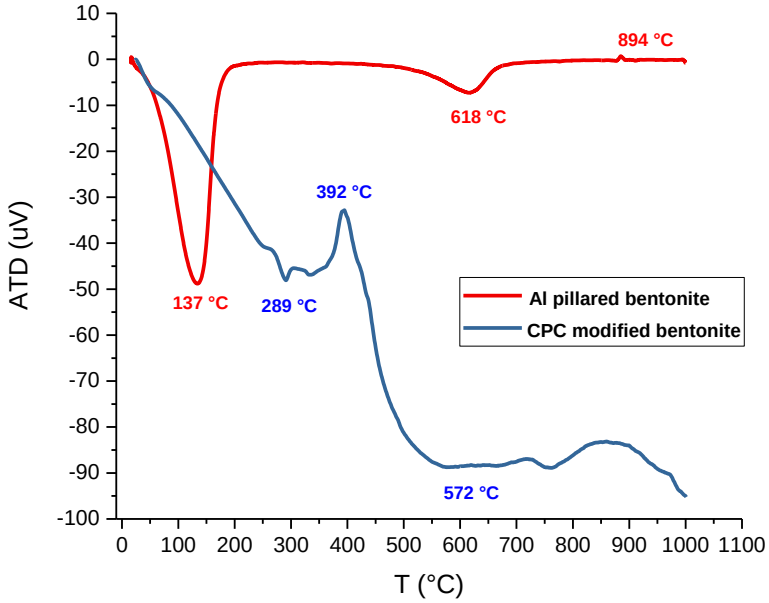

Figure 4. Differential thermal analysis (DTA) curves for B-Al-PILC and B-CPC

In the area of low temperatures (Figure 4), the existence of an intense endothermic phenomenon at 137°C, which corresponds to the loss of adsorbed water on the material (6.73%) that is less than that of the natural clay (13.88%) is due to the lower presence of exchangeable cations in the hydrated inter-layer sheets. Dehydroxylation that continues between 337 °C and 650 °C is also detected at about 620 °C in an important step. In the second and third stage (620 °C and 822 °C), there is a consistent weight loss (8.15%) from the un-hydroxylation of polyhydroxy cationsOH groups and from the total dehydroxylation of the structure of the prepared surface. This step is related to the stability of the pillars, a significant decrease in basal spacing values, which occurs at this temperature, indicates the collapse of the clay structure. Therefore, the thermos-gravimetric analyses are in agreement with the aforementioned thermal stability of the synthesized pillared clay up to 822 °C. The TGA & DTA measurements were performed to clarify the contribution of CPC amount to hydrophobicity of clay samples modified by CPC surfactant (Figure 2 and Figure **4**). Desorbing the adsorbed water B-CPC was not obvious because the hydrophobicity enhanced by modifying the outer surface of the support. Weight loss (24.62%), due to the decomposition of the CPC of the outer surface of the support is in the temperature area between 225 and 415 ° C. A significant loss of mass (16.13%) from 440-750 °C was observed due to degradation and evaporation of CPC intercalated between the clay layers. Ignoring the contribution of the adsorbed water, CPC content weight in the B-CPC was calculated at 40.75%, with 40% in the interlayer surface and 60% in the external surface, suggesting different configurations of CPC on the surface of the clay. CPC molecules laying in bilayer on the interlayer surface of bentonite clay and in perpendicular monolayer on the external surface of bentonite clay.

3-3.Infra-Red Characterization.

Examination of the infrared absorption spectra (Figure 5 and Figure **6**) samples of crude and purified bentonite shows absorption bands that we present as follows [43-45]. The spectra show two absorption bands located between 3200 and 3800 cm^{-1} and between 1600 and 1700 cm^{-1}. The band that stretches between 1600 and 1700 cm^{-1} is attributed to stretching vibrations of OH constitution water plus water adsorbed binding vibrations. The band in the range of 3200-3800 cm^{-1} with a strong peak and peak shoulders at 3621 and 3435 cm^{-1} that characterizes the montmorillonite and corresponds to the stretching vibrations of the OH groups of the octahedral layer is coordinated at Al + Mg (3640 cm^{-1}) or Al 2 (3600 cm^{-1}). H_2O molecules deformation vibrations are characterized by the band 3400 cm^{-1}. The band centered about 1630 cm^{-1} is attributed to deformation vibrations of the molecules of H_2O adsorbed between the sheets.

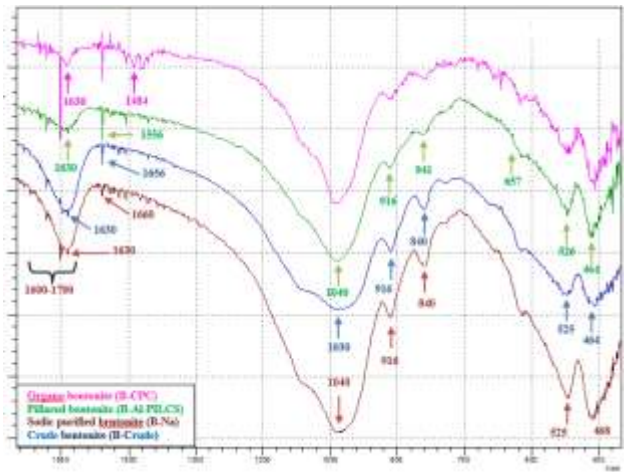

Figure 5. Infrared spectrum analysis of clays studied in [1800-400].

The intense band situated between 900 and 1200 cm^{-1} and centred around 1030 cm^{-1} corresponds to stretching vibrations of the Si-O bond. In the purified clay (B-Na purified), it is situated around 1040 cm^{-1} between 1115 and 1020 cm^{-1}. The bands situated at 525, 468 and 425 cm^{-1} are assigned respectively to the connections of the deformation vibrations Si-O-Al, Mg-Si-O and Si-O-Fe. For pillared clay (B-Al-PILC) in high frequency areas of the infrared spectrum (Figure 6) the bands corresponding to water molecules present in the intermediate layers and the structural hydroxyl groups in the clay layers have been observed in the area between 3350 to 4000 cm^{-1}.

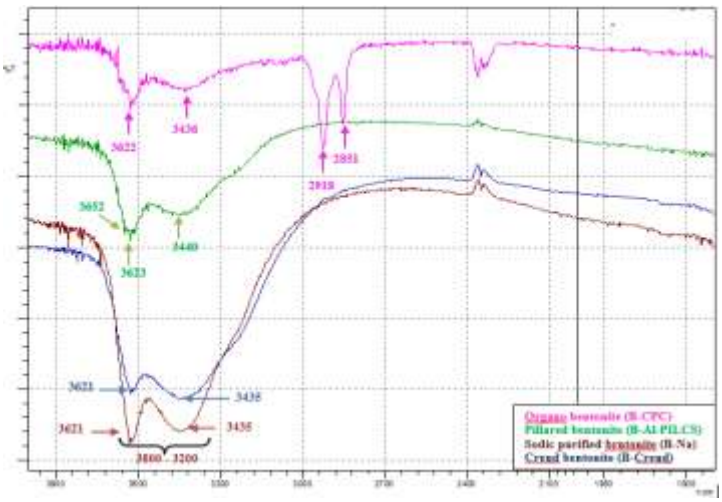

Figure 6. Infrared spectrum analysis of clays studied between [3800-1800].

The absorption band at 3440 cm^{-1} corresponds to the symmetrical stretching vibration of OH water bound [46]. In addition, it can be observed that the intensity is dependent on the type and the concentration of the interlayer cations. For B-Al-PILCs, the band locates at 3623 cm^{-1} and the intensity is lower than that of purified Na B-3621 cm^{-1}. The former is ascribed to the OH stretching vibration in hydroxyl-Al cations while the latter corresponds to the hydroxyl groups involved in water-water hydrogen bands [45]. For B-Al-PILCs sample, a new band situated at 3652 cm^{-1}, which is probably produced by the change in position of the Si-OH group in the structure of the smectite. The original position was altered by the entrance of the aluminium ion in the smectite structure, which is likely to be due to Si-OH species perturbed by pillars, and designated as SiOH*. The low frequency regions of the infrared spectra of the purified B-Na and B-Al-PILCs are very similar, but the latter shows a very low intensity band at 550-450 cm-1originated from Si-O bending and Al-O stretching vibrations. There was no change in Si-O bending, except a slight Al-O stretching, and an increase in the intensity due to pillaring phenomenon. This situation was supported by the increase in Al content around 657 cm^{-1}. The lattice vibration at 657 cm^{-1} can be ascribed to the Al-O bond of tetrahedrally coordinated Al^{3+} cations in the center of the Al_{13} pillars [47]. The band center of B-Al-PILCs is situated at 1556 cm^{-1} with a higher intensity compared to that of B-Na purified at 1560 cm^{-1}. This should be attributed to an increase of water content in B-Al-PILCs, resulting from the intercalation of hydroxyl-Al cations into the clay interlinearspace. Symmetrical and asymmetrical features stretching vibration of C-H particles 2918, 2851 and 1484 cm^{-1} were assigned to the CPC intercalation in the clay interlayers [48]. Moreover, we note that the vibration bands and bending vibration peak belonging to H-O-H in the spectra of B-Na purified B-Crude and B-Al-PILCs, in 3435, 3440 and 1630 cm^{-1}, respectively almost disappeared in the case of B-CPC. This shows that B-CPC adsorbs less water than B-Na purified B-Al-PILCs and B-Crude and this explains the hydrophobicity of this support.

3-4.Textural Measurements (Determination of Specific Surface Area by BET).

These analyses were done in order to determine the influence of chemical modification of clays (B-Na, B-CPC and B-Al-PILC) on their structural characteristics. Before analyses the samples were automatically degassed under vacuum for 4 h at 475 K; the samples mass used are 0.1318 g and 0.1438 g of samples. The adsorption-desorption isotherms are important due to the parameters that can be established: specific surface area, porosity, pore volume, pore size distribution and average pore diameter. More, we can also obtain qualitative information regarding the structure (pores shape, inter-connexions …etc). To determine the textural characteristics several models are proposed [38]. In order to determine the textural properties, the Langmuir model in a range of relative pressure smaller than 0.07 [49], and the correction to the BET model proposed by [50] were used. The microporous areas were determined by curves using the De Boer's method, and the micropore volumes were determined by curves using the Harkin-Jura equation. The nitrogen adsorption-desorption isotherms of the raw bentonite, sodium bentonite (B-Na purified),) the pillared bentonite (B-Al-PILCs), and the organic bentonite (B-CPC) are shown in figure 7 and Figure **8**. The comparison between the three isotherms, lead to a type IV isotherm with H1 hysteresis for ther raw and the B-Na purified [51] and H4 hysteresis for the B-Al-PILCs and H3 hysteresis for the B-CPC. In the case of the raw and the sodium purified bentonite (B-Na), the H1 form of hysteresis is often associated with adsorbents made up of agglomerates and aggregated plane particles forming slit shape and narrow with regular size distribution of the pores. The raw and Na-bentonites are porous materials, with mesopores between interlayers. The increase in the adsorption of N_2 of the B-Al-PILCs in comparison to that of the B-Na purified results from the porosity generated by the pillaring process. The pillared bentonite B-Al-PILCs present developed mesoporosity and the hysteresis has a narrow loop with two branches which are almost horizontal and nearly parallel. Type I isotherm of the B-Al-PILCs is due to the azote uptake

by the accessible micropore volume. By t-plot calculation, the surface area of micropores is about 186 m^2/g. The measurement of textural properties confirms the results of the XRD. The increase in micro-porosity obtained with the pillaring, indicates that the Al_{13} pillars could occupy a greater fraction of the interlinear spaces. For the B-CPC organophilic bentonite the interlayer sheets are collapsed by the the van der waals intercations of the surfactant alkyl chains. The surfactant molecules on the extenal surface agglomerate giving macropores materials in solide phase.
Relevant data for the the bentonite clays are presented in Table 1.

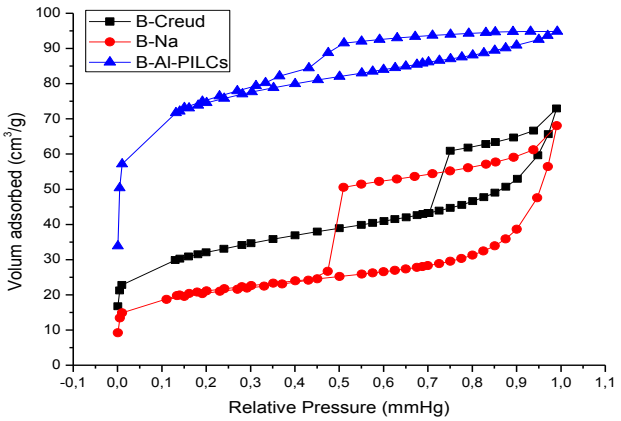

Figure 7. Nitrogen adsorption-desorption isotherm of the raw bentonite (B-raw), sodium bentonite (B-Na) and pillared bentonite (B-Al-PILCs).

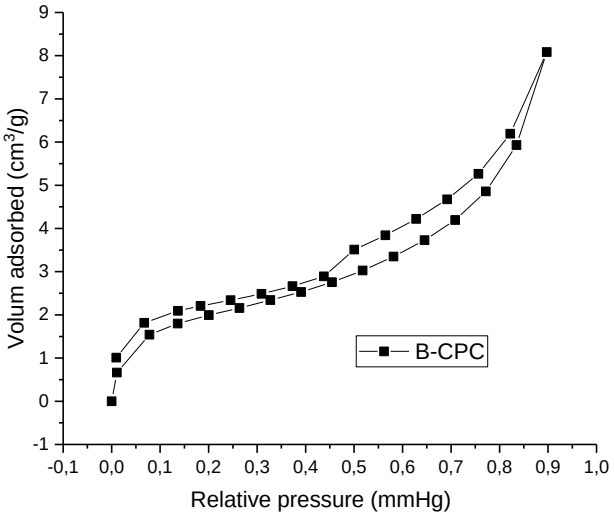

Figure 8. Nitrogen adsorption-desorption isotherm of the organic bentonite (B-CPC).

Table 1. Selected textural properties of the investigated clays.

Samples	**S_{BET} (m^2/g)**	**S_{ext} (m^2/g)**	**$V_{0,991}$ (cm^3/g)**	**V_{mic} (cm^3/g)**	**D_{med} (Å)**
B-Na Purified	107,5	81,024	0,123	0,053	5,32
B-Na Brute	70,2	32,67	0,089	0,036	5,76
B-Al-PILC	270,4	83,68	0,246	0,147	8,9

B-CPC	7,2	6,67	-	$1,61.\ 10^{-4}$	14

The B-AL-PILCs surface area is determined primarily by the microporous region (Table 1), which is obvious to a significant change in the texture of B-Na purified. Table 1 indicates that as a result of the pillaring process, the determined BET surface area (S_{total}) of the sodium clay (B-Na) increased from 107,5 m²/g to 270,4 m²/g for B-AL-PILCs. In the case of B-AL-PILCs, the internal surface constitute 70% of the total surface whereas in the case of B-Na bentonite the internal surface is about 25%, because the interaction between interlayers are very strong to collapse the sheets and prevent the internal adsorption of nitrogen gas molecules. This internal surface is accessible for ethylene glycol adsorption [52]. On the contrary, for the B-CPC clay, a value of 7,2 m²/g was obtained which is due to the fact that the surfactant occupied the available adsorption sites, so only external surface is practically valable for the nitrogen adsorption. In regards to the porosity, Table 1 shows that B-Al-PILCs has an average pore radius of 8,9 Å wich is equivalent to the thikness of one Al_{13} pillars, and it can be classified as a microporous material (19, 24). As mentioned in the previous discussion, the used samples of natural clay, the B-CPC were not micrporous. Also for the B-CPC the inerlayers (microporosity) are filled by the organic molecules.

4.Conclusion.

The resultant modified bentonite complexes were characterised using FTIR, with a combination of XRD, and textural analysis. The Nador bentonite has been successfully modified using the inorganic cations of Al_{13} resulting in pillared bentonite and organic cations of CPC surfactant molecules giving organoclay bentonite. Results obtained from FTIR spectra showed that there were changes in the clay structure with Al pillaring and CPC intercalation. The XRD patterns show that the basal spacing of the complexes increase to 19 Å for B-AL-PILCS and 21,7 Å for B-CPC. The insertion of pillars, which caused a slighter increase in the clay spacing. Its specific surface area is about three times larger than that of the parent Na-montmorillonite due principally to the creation of a remarkable microporous network[53]. The Al pillared clays are thermally stable up to 650°C and the organophilic clays are unstable by heating up to 220°C. Concerning the textural results, the pillared B-AL-PILCS is microporous material and presents a developed meso-porosity open to penetration by gaseous azote adsorbent. The organophilic clay B-CPC is non-microporous with low meso-porosity and the clay interlayers were filled with the organic cations. The determined surface area (S_{total}) of the sodium clay (B-Na) increased from 107 m²/g to 270 m²/g for B-AL-PILCs, and decreases considerably for B-CPC to 7 m²/g. The results obtained reveal that the insertion of alumina pillar increase the surface are and the porosity of the clay, however the intercalation with cationic CPC molecules reduces the surface area and the porosity leading to only the external surface area accessible to the N_2 gas adsorption.

References

[1] C. Tcheka *et al.*, *Moroccan Journal of Chemistry,* vol. 6, no. 3, pp. 6-3 (2018) 525-539, 2018.

[2] A. Olaya, S. Moreno, and R. J. A. C. A. G. Molina, vol. 370, no. 1-2, pp. 7-15, 2009.

[3] G. W. Brindley and R. E. Sempels, *Clay Minerals,* vol. 12, pp. 229-237, 1977.

[4] R. M. Barrer, "Shape-Selective Sorbents Based on Clay Minerals," *Clays Clay Minerals,* vol. 37, pp. 381-395, 1989.

[5] F. Bergaya, N. Hassoun, J. Barrault, and L. Gatineau, *Clay Minerals,* vol. 28, pp. 109-122, 1993.

[6] F. Bergaya, *CEA-PLS Newsletter,* vol. 7, pp. 11-12, 1994.

[7] K. Beneke, P. Thiesen, and G. Lagaly, *Inor-ganic Chemistry,* vol. 34, pp. 900-907, 1995.

[8] T. J. Pinnavaia, M. S. Tzou, S. D. Landau, and R. H. Raythatha, *Journal of Molecular Catalysis,* vol. 27, pp. 195-212, 1984.

[9] N. Lahav, U. Sham, and J. Shabtai, *Clays Clay Minerals,* vol. 26, pp. 107-115, 1978.

[10] F. Bergaya, *Journal of Porous Materials*, vol. 2, pp. 91-96, 1995.
[11] A. Tahani *et al.*, *Journal of Chemical Physics*, vol. 96, pp. 464-469, 1999.
[12] C. Cooper and R. Burch, *Water Research*, vol. 33, pp. 3689-3694., 1999.
[13] T. G. Danis, T. A. Albanis, D. E. Petrakis, and P. J. Pomonis, *Water Research*, vol. 32, pp. 295-302, 1998.
[14] A. Dyer and V. T. Gallardo, Springer, Dordrecht. ed. Berlin: Springer Netherlands, 1990.
[15] A. Dyer, V. T. Gallardo, and C. W. Roberts, in *Zeolites, Facts, Figures, Future*, 1989.
[16] I. K. Konstantinuo, T. A. Albanis, D. E. Petrakis, and P. J. Pomonis,*Water Research*, vol. 34, pp. 3123-3136, 2000.
[17] R. G. Osorio, V. T. Gallardo, C. S. López, and C. S. Arellano, *Drying Technology*, vol. 24, no. Osorio-Revilla, G., Gallardo-Velázquez, T.,, pp. 1033-1038, 2006.
[18] G. D. Theopharis, A. A. Triantafyllos, E. P. Dimitrios, and J. P. Philip, *Water Research*, vol. 32, pp. 295-302, 1998.
[19] A. Nennemann *et al.*, *Applied Clay Science*, vol. 18, pp. 265-275, 2001.
[20] Y.-M. Jeon, J. Kim, D. Whang, and K. J. J. o. t. A. C. S. Kim, *Journal of the American Chemical Society,*, vol. 118, no. 40, pp. 9790-9791, 1996.
[21] Y. Xi, M. Mallavarapu, and R. Naidu, *Applied Clay Science*, vol. 48, no. 1-2, pp. 92-96, 2010.
[22] C. C. López, R. G. Osorio, V. T. Gallardo, and C. S. Arellano, *Canadian Journal of Chemistry*, pp. 305-311, 2008.
[23] P. Lagas, *Chemosphere*, vol. 17, pp. 205-216, 1988.
[24] L. Z. Zhu, X. G. Ren, and S. B. Yu, *Environmental Science & Technology*, vol. 32, pp. 3374–3378, 1998.
[25] C. C. Wang, L. C. Juang, C. K. Lee, T. C. Hsu, J. F. Lee, and H. P. Chao, *Journal of Colloid and Interface Science*, vol. 280, pp. 27–35, 2004.
[26] N. Yilmaz and S. Yapar, *Applied Clay Science*, vol. 27, pp. 223–228, 2004.
[27] O. Regev and A. Khan, *Applied Clay Science*, vol. 182, pp. 95–109, 1996.
[28] Y. H. Shen, *Chemosphere*, vol. 44, pp. 989–995, 2001.
[29] S. Xu and S. A. Boyd, *Langmuir*, vol. 11, p. 2508, 1995.
[30] B. Xing, J. J. Pignatello, and B. Gigliotti, *Environmental Science & Technology*, vol. 30, p. 2432, 1996.
[31] K. R. Srinivasan and H. S. Fogler, *Clays & Clay Minerals*, vol. 38, pp. 277-286, 1990.
[32] M. R. Stackmeyer, *Applied Clay Science*, vol. 6, pp. 39–57, 1991.
[33] L. Z. Zhu, B. L. Chen, and X. Y. Shen, *Environmental Science & Technology*, vol. 34, pp. 468–475, 2000.
[34] B. K. G. Theng, G. J. Churchman, W. P. Gates, and G. Yuan, *Organically modified clays for pollutant uptake and environmental protection*. Berlin: Springer-Verlag, 2008.
[35] S. S. Ray and M. Okamoto, *Progress in Polymer Science*, vol. 28, pp. 1539–1641, 2003.
[36] J. A. Smith and A. Galan, *Environmental Science & Technology*, vol. 29, pp. 685–692, 1995.
[37] M. Aalaoul, A. Azdimousa, and K. El Hammouti, *JOURNAL OF MATERIALS*, vol. 6, no. 12, pp. 3564-3573, 2015.
[38] N. Platon *et al.*, *Revista de Chimie (Bucharest)*, vol. 62, pp. 799-805, 2011.
[39] M. H. Y. Touati, M. Jandoubi, M. B. Amor, and M. Z. Benna, *Moroccan Journal of Chemistry*, vol. 6, no. 1, pp. 135-147, 2018.
[40] X. Y. Feng, G. J. Hu, X. F. Meng, Y. F. Ding, S. M. Zhang, and M. S. Yang, *Applied Clay Science*, vol. 45, pp. 239–243, 2009.
[41] S. I. Marras, A. Tsimpliaraki, I. Zuburtikudis, and C. Panayiotou, *Journal of Colloid and Interface Science*, vol. 315, pp. 520–527, 2007.
[42] X. Zixian , L. Fengzhu , Z. Yihe , and F. Liling *Chemical Engineering Journal*, vol. 215, pp. 755–762, 2013.
[43] V. C. Farmer, *Infrared spectroscopy*. Oxford: Pergamon Press, 1979.
[44] P. Salerno, M. B. Asenjo, and S. Mendioroz, *Thermochimica Acta*, vol. 379, pp. 101-109, 2001.

[45] J. Madejova, M. Janek, P. Komadel, H. J. Herbert, and H. C. Moog, *Applied Clay Science*, vol. 20, pp. 255-271, 2002.

[46] W. Xue, H. He, J. Zhu, and P. Yuan, *Spectro-chimica Acta Part A: Molecular and Biomolecular Spectroscopy,* vol. 67, pp. 1030-1036, 2007.

[47] J. F. Xiao, Y. Hu, Z. Z. Wang, Y. Tang, Z. Y. Chen, and W. C. Wei, *European Polymer Journal*, vol. 41, pp. 1030–1035, 2005.

[48] I. Deniau, "Caractérisation géochimique du kérogène associé à l'argile oligocène de Boom (Mol, Belgique) et évolution sous divers stress thermiques," Thèse de Doctorat, Chimie ParisTech, Paris, 2002.

[49] S. J. Gregg and S. W. Sing, "Adsorption, Surface Area and Porosity," *Journal of The Electrochemical Society,* 1982.

[50] M. J. Remy, A. C. V. Coelho, and G. Poncelet, *Microporous Materials,* vol. 7, pp. 287-297, 1996.

[51] P. Bankoviæ , N. Milutinoviæ, A. Rosiæ, and N. J. Jovièiæ, " *Russian. Journal of Physical Chemistry,* vol. 83, p. 1485, 2009.

[52] M. El Miz, H. Akichoh, D. Berraaouan, S. Salhi, and A. Tahani, ," *American Journal of Chemistry,* vol. 7, no. 4, pp. 105-112, 2017.

[53] H. Rezala, J. L. Valverde, A. Romero, A. Molinari, and A. Maldotti, ," *Moroccan Journal of Chemistry,* vol. 3, no. 2, pp. 3-2 (2015) 314-330, 2015.